# Comparative Investigation of the Spin-Crossover Compounds $Fe(btz)_2(NCS)_2$ and $Fe(phen)_2(NCS)_2$ (Where btz = 2,2′-Bi-4,5-dihydrothiazine and phen = 1,10-Phenanthroline). Magnetic Properties and Thermal Dilatation Behavior and Crystal Structure of $Fe(btz)_2(NCS)_2$ at 293 and 130 K

**José-Antonio Real,*[1a] Bernard Gallois,*[1b] Thierry Granier,[1b] Franz Suez-Panamá,[1b] and Jacqueline Zarembowitch*[1c]**

Departament de Química Inorgánica, Universitat de València, 46100 Burjassot, Spain, Laboratoire de Cristallographie et de Physique Cristalline (URA 144, CNRS), Université de Bordeaux I, 33405 Talence, France, and Laboratoire de Chimie Inorganique (URA 420, CNRS), Université de Paris-Sud, 91405 Orsay, France

*Received January 24, 1992*

The crystal structure of $Fe(btz)_2(NCS)_2$ (**1**) was determined by X-ray diffraction at ≈293 and ≈130 K in order to detect the structural changes associated with the spin transition. The space group is *Pbcn* with $Z = 4$ at both temperatures. Lattice constants are as follows: $a = 13.2880$ (11) Å, $b = 10.8610$ (11) Å, and $c = 16.9199$ (19) Å at ≈293 K and $a = 13.0551$ (17) Å, $b = 10.6504$ (17) Å, and $c = 16.6717$ (39) Å at ≈130 K. The data were refined to $R = 0.059$ (0.062) at ≈293 K (≈130 K) for 1102 (1095) observed independent reflections ($(F_o)^2 > 2.5\sigma(F_o)^2$). These results compare with those previously reported for $Fe(phen)_2(NCS)_2$ (**2**). However, the temperature dependence of $\chi_M T$ ($\chi_M$ = molar magnetic susceptibility and $T$ = temperature) is different for the two compounds: **2** shows a very abrupt singlet ↔ quintet spin conversion and **1** a gradual one. At the molecular scale, the structural modifications associated with the spin change are also found to be similar in **1** and **2**; they mainly consist in a large reorganization of the iron(II) environment: when the temperature is lowered from 293 to 130 K, the Fe–N(L) (L = btz, phen) and Fe–N(CS) distances decrease by 0.20 (mean value) and 0.10–0.11 Å, respectively, and a noticeable variation of the N–Fe–N angles, leading to a more regular shape of the [Fe–$N_6$] octahedron, is observed. Moreover, in both compounds, the molecular packing may be described as sheets of molecules parallel to the a–b plane. However, the framework of the intermolecular interactions is different in **1** and **2**, and the reinforcement of these interactions upon the high-spin → low-spin conversions is more pronounced between consecutive sheets in **1** and between molecules of the same sheet in **2**, leading to a higher bidimensional character for the latter compound. This difference in structural anisotropy, which might be at the origin of the difference in cooperativity of the two spin transitions, is reflected on the thermal variation of the lattice parameters measured for both complexes in the 130–293 K temperature range: in **1**, all the parameters evolve continuously; in **2** the evolution of the $a$ and $b$ parameters clearly shows a discontinuity in the close vicinity of the spin transition, whereas the $c$ parameter varies continuously. The values found for the total variation of the unit cell volume are of the same order of magnitude for the two compounds: $\Delta V = 124$ Å$^3$ for **1** and 119 Å$^3$ for **2**. The same holds for the values of the component $\Delta V_{SC}$ (which corresponds to the spin-crossover alone), estimated at 89 Å$^3$ for **1** and 72 Å$^3$ for **2** in the case of a complete spin conversion.

## Introduction

Most of the investigations concerning thermally-induced or pressure-induced electronic spin crossovers, reported to date, relate to iron(II), iron(III) and cobalt(II) complexes.[2] Spin conversions were observed as well in the solid state as in solution. In the latter case,[2i,3] the process is essentially molecular, owing to the isolation of molecules which precludes long-range order: the spin conversion is gradual and does not present a hysteresis effect. In the solid state,[4] the situation is usually quite different, for the phenomenon has a cooperative character resulting from lattice effects: the stronger the cooperativity, the more abrupt the transition is.

Several theoretical attempts to interpret the cooperative transitions have been proposed.[5] The coupling parameter utilized to account for cooperative effects is generally treated implicitly or phenomenologically and hence cannot provide any information on the transition mechanism. On the other hand, a number of experimental studies carried out with a view to better understand this mechanism were reported. The present work was developed along this line. Its purpose is to detect molecular and crystal

(1) (a) Universitat de València. (b) Université de Bordeaux I. (c) Université de Paris-Sud.

(2) (a) Barefield, E. K.; Busch, D. H.; Nelson, S. M. *Q. Rev.* **1968**, *22*, 457. (b) König, E. *Coord. Chem. Rev.* **1968**, *4*, 471. (c) Martin, R. L.; White, A. H. *Transition Met. Chem. (N.Y.)* **1968**, *4*, 113. (d) Goodwin, H. A. *Coord. Chem. Rev.* **1976**, *18*, 293. (e) Sacconi, L. *Pure Appl. Chem.* **1971**, *27*, 161. (f) Gütlich, P. *Struct. Bonding (Berlin)* **1981**, *44*, 83. (g) König, E.; Ritter, G.; Kulshreshtha, S. K. *Chem. Rev.* **1985**, *85*, 219. (h) Rao, C. N. R. *Int. Rev. Phys. Chem.* **1985**, *4*, 19. (i) Toftlund, H. *Coord. Chem. Rev.* **1989**, *67*, 108. (j) Zarembowitch, J. *New J. Chem.* **1992**, *16*, 255 and references therein.

(3) (a) Beattie, J. K. *Adv. Inorg. Chem.* **1988**, *32*, 2 and references therein. (b) McGarvey, J. J.; Lawthers, I.; Heremans, K.; Toftlund, H. *Inorg. Chem.* **1990**, *29*, 252.

(4) (a) Sorai, M.; Seki, S. *J. Phys. Chem. Solids* **1974**, *35*, 555. (b) Gütlich, P.; Hauser, A. *Coord. Chem. Rev.* **1990**, *97*, 1. (c) König, E. *Prog. Inorg. Chem.* **1987**, *35*, 527. (d) Ozarowsky, A.; McGarvey, B. R.; Sarkar, A. B.; Drake, J. E. *Inorg. Chem.* **1988**, *27*, 628. (e) Gallois, B.; Real, J. A.; Hauw, C.; Zarembowitch, J. *Inorg. Chem.* **1990**, *29*, 1152. (f) Claude, R.; Real, J. A.; Zarembowitch, J.; Kahn, O.; Ouahab, L.; Grandjean, D.; Boukheddaden, K.; Varret, F.; Dworkin, A. *Inorg. Chem.* **1990**, *29*, 4442. (g) König, E. *Struct. Bonding (Berlin)* **1991**, *76*, 51.

(5) (a) Bacci, M. *Coord. Chem. Rev.* **1988**, *86*, 245 and references therein. (b) Slichter, C. P.; Drickamer, H. G. *J. Chem. Phys.* **1972**, *56*, 2142. (c) Gütlich, P.; Köppen, H.; Link, R.; Steinhauser, H. G. *J. Chem. Phys.* **1979**, *70*, 39. (d) Spiering, H.; Meissner, E.; Köppen, H.; Müller, E. W.; Gütlich, P. *Chem. Phys.* **1982**, *68*, 65. (e) Purcell, K. F.; Edwards, M. P. *Inorg. Chem.* **1984**, *23*, 2620.

0020-1669/92/1331-4972$03.00/0 

parameters which might play a role in spin-conversion cooperativity, on the basis of a comparative X-ray diffraction investigation of two iron(II) complexes, one exhibiting a discontinuous spin-crossover and the other a gradual one.

Some years ago, Bradley and colleagues[6] reported the results of a magnetic and Mössbauer-effect investigation on a series of $FeL_2(NCS)_2$ spin-crossover complexes, L being 2,2'-bithiazoline (bt), 2,2'-bi-4,5-dihydrothiazine (btz) or alkyl-substituted derivatives. $Fe(bt)_2(NCS)_2$ showed a very sharp spin transition and has been widely investigated. Mössbauer spectrometry,[7] powder X-ray diffraction,[7] magnetic susceptibility measurements,[8] and calorimetry[9] revealed the first-order character of the phase transition. More recently, further investigations have been performed on this compound: an X-ray single-crystal structure of the high-spin isomer (at room temperature),[4d] an EPR study of dopped single crystals,[4d] and the LIESST effect in the pure complex.[10] On the contrary, less attention has been devoted to $Fe(btz)_2(NCS)_2$, probably because this compound shows a gradual spin equilibrium with residual paramagnetism and diamagnetism in the low- and room-temperature regions, respectively.

In this paper we firstly report the single-crystal X-ray diffraction structure of $Fe(btz)_2(NCS)_2$ both at room temperature and 130 K and the variable temperature magnetic behavior of a polycrystalline sample of the same origin as the crystal used for X-ray experiments. Since this compound is found to be isostructural with the crystalline form II of $Fe(phen)_2(NCS)_2$,[4e] which exhibits an abrupt spin transition, the two complexes provide a good example to compare the well-established main classes of spin-crossover behaviors (discontinuous and gradual).[2g] So the temperature dependence of lattice parameters and unit cell volume are also reported for both compounds and discussed in order to find ways to better understand the spin-transition cooperative mechanism.

## Experimental Section

**Synthesis. 2,2'-Bi-4,5-dihydrothiazine (btz).** Dithiooxamide (41.67 mmol) was reacted with 2-aminopropanol (83.34 mmol) in ethanolic solution (200 mL) at room temperature over night. The brown solution was evaporated until about 40 mL to form *N,N'*-bis(2-hydroxypropyl)-dithiooxamide which was filtered, then recrystallized from ethanol. A suspension of this compound in toluene (29.66 mmol, 200 mL) was reacted with an excess of thionyl chloride (65 mmol), forming 2,2'-bi-4,5-dihydrothiazoline dihydrochloride which was filtered off and neutralized with an aqueous solution of sodium bicarbonate, yielding btz, which was purified by soxhlet extraction with hexane, followed by crystallization from acetone. A white crystalline product was obtained (yield ≈ 20%).[11,12] NMR data, performed in $CD_3Cl$: $^1H$ = triplet at $\delta$ = 3.87 ppm (–S–$CH_2$–), $J_{HH} \approx 5$ Hz; triplet at $\delta$ = 2.95 ppm (=N-$CH_2$–), $J_{H-H} \approx 5$ Hz and pentet at $\delta$ = 1.85 ppm (–C–$CH_2$–C–), $J_{H-H} \approx 6$ Hz. $^{13}C$: four singlets at 158, 47.31, 25.29, and 19.15 ppm.

**$Fe(btz)_2(NCS)_2$ (1).** A btz solution (0.5 mmol), prepared in methanol (20 mL), was added dropwise with stirring to a hot methanolic solution of $Fe(pyridine)_4(NCS)_2$ (0.25 mmol; 50 mL). The solid which formed rapidly was filtered and purified by soxhlet extraction (yield ≈ 90%). Black shining crystals were obtained in this process and characterized by a single-crystal X-ray technique. All the manipulations were carried out under an argon stream.

**$Fe(phen)_2(NCS)_2$ (2).** This compound was prepared, in the crystalline form II, as previously described.[4e]

**Magnetic Susceptibility Measurements.** These measurements were performed on a crystalline sample of **1** weighing 5.63 mg, over the temperature range 295–100 K, by using a Faraday-type magnetometer equipped with an Oxford Instruments continuous-flow cryostat. The independence of the susceptibility with regard to the applied magnetic field was checked at room temperature. $HgCo(NCS)_4$ was used as a susceptibility standard. The diamagnetism correction was estimated, from Pascal's constants,[13] to be $201 \times 10^{-6}$ cm$^3$ mol$^{-1}$. The uncertainty in the temperature is about 0.1 K.

**Table I.** Crystallographic Data for Compound **1**[a]

| | | | |
|---|---|---|---|
| chem formula | $C_{18}H_{24}N_6S_6Fe$ | space group | *Pbcn* |
| fw | 572.6 | $T$, K | 293 |
| $a$, Å | 13.2880 (11) (13.0551 (17)) | λ, Å | 1.541 78 |
| $b$, Å | 10.8610 (11) (10.6504 (17)) | $\rho_{calcd}$, g cm$^{-3}$ | 1.557 (1.640) |
| $c$, Å | 16.9199 (19) (16.6717 (39)) | $\mu$, cm$^{-1}$ | 97.888 (103.116) |
| $V$, Å$^3$ | 2441.9 (2318.1) | $R$ | 0.059 (0.062) |
| $Z$ | 4 | $R_w$ | 0.057 (0.064) |

[a] Values at 130 K are given in parentheses. [b] $R = \sum[|F_o| - |F_c|]/\sum|F_o|$; $R_w = \sum w^{1/2}[|F_o| - |F_c|]/\sum w^{1/2}|F_o|$.

**X-ray Diffraction Experiments.** Preliminary X-ray investigations were performed at room temperature by the usual photographic methods in order to check the good quality of the crystals and to determine the space group in which **1** crystallizes. For this latter complex, additional reciprocal lattice photographs recorded at low temperature (130 K) do not show any extra spot in spite of a long exposure time. Symmetries in the diffraction patterns and systematic extinctions indicate that the space group is, as already observed for compound **2**, orthorhombic (*Pbcn*) over the whole temperature range.

The temperature dependence of the lattice parameters in the range 130–293 K (for both compounds) as well as the intensity data collections (for **1**) were obtained on an Enraf Nonius CAD-4 diffractometer with monochromatized Cu K$\alpha$ radiation. Crystal cooling was achieved by a cold nitrogen gas flow surrounded by a jacket of dry nitrogen gas at room temperature so as to prevent frost from growing around the sample. The temperature fluctuation is assumed to be less than ±2 K down to 130 K.

Lattice parameters were obtained by a least-squares refinement of the angular positions of 22–25 centered Bragg reflections ($10° \le \theta \le 35°$). All data have been recorded during a single temperature loop: cooling down to 130 K and warming up to 293 K.

The **1** and **2** crystals were black plate-shaped single crystals of sizes $0.05 \times 0.11 \times 0.22$ mm and $0.06 \times 0.15 \times 0.25$ mm, respectively.

Details on crystal data collection and structure refinements relative to **1** are summarized in Table I. The intensities of 1789 ($T \approx 293$ K) and 1697 ($T \approx 130$ K) independent Bragg reflections ($1.0° \le \theta \le 35°$, $h_{max} = 11$, $k_{max} = 14$, $l_{max} = 18$) were collected by $\omega/2\theta$ scans. Lorentz polarization and absorption corrections have been applied. A total of 1102 ($T \approx 293$ K) and 1095 ($T \approx 130$ K) reflections for which $(F_o)^2 \ge 2.5\sigma(F_o)^2$ were used to refine the structure.

At room temperature, the complete structure was solved by Fourier recycling, using the program MITHRIL.[14] At both temperatures (293, 130 K), the full-matrix refinements, based on $F_o$, were carried out using the program SHELX 76.[15] The final atomic coordinates, obtained at room temperature, were used as starting values in the low-temperature refinement. Atomic scattering factors were taken from ref 16. Final refinement minimizing $\sum w([|F_o| - |F_c|])^2$ converged at $T \approx 293$ K to $R = \sum[|F_o| - |F_c|]/\sum|F_o| = 0.059$ (0.062 at $T \approx 130$ K) and $R_w = \sum w^{1/2}[|F_o| - |F_c|]/\sum w^{1/2}|F_o| = 0.057$ (0.064 at $T \approx 130$ K). Non-hydrogen atoms were refined anisotropically. The goodness of fit values are 1.05 and 1.21 at $T \approx 293$ K and $T \approx 130$ K respectively. Fractional atomic coordinates and equivalent isotropic thermal parameters are given in Table II for $T \approx 293$ K and $T \approx 130$ K.

## Results

**Magnetic Properties.** Magnetic susceptibility measurements were performed, first at decreasing and then at increasing temperatures, on a sample constituted by small crystals of **1**. The

(6) Bradley, G.; McKee, V.; Nelson, S. M. *J. Chem. Soc., Dalton Trans.* **1978**, 522.
(7) König, E.; Ritter, G.; Irler, W.; Nelson, S. M. *Inorg. Chim. Acta* **1979**, *37*, 169.
(8) Müller, E. W.; Spiering, H.; Gütlich, P. *Chem. Phys.* **1983**, *79*, 1439.
(9) Kulshreshtha, S. K.; Sasikala, R.; König, E. *Chem. Phys. Lett.* **1986**, *123*, 215.
(10) Figg, D. C.; Herver, R. H. *Inorg. Chem.* **1990**, *29*, 2170.
(11) Nelson, J.; Nelson, S. M.; Perry, W. D. *J. Chem. Soc., Dalton Trans.* **1976**, 1282.
(12) Tomalia, D. A.; Paige, J. N. *J. Org. Chem.* **1973**, *38*, 3949.
(13) Mulay, L. N.; Boudreaux, E. A. *Theory and Application of Molecular Paramagnetism*; Wiley: London, 1976.
(14) Gilmore, C. J. *J. Appl. Crystallogr.* **1984**, *17*, 42.
(15) Sheldrick, G. M. *SHELX76 System of Computing Programs*; University of Cambridge: Cambridge, England, 1976.
(16) *International Tables for X-Ray Crystallography*, Kynoch Press: Birmingham, England, 1974; Vol. 4, p 99.

**Table II.** Atomic Coordinates (× $10^4$)[a] and Isotropic Thermal Parameters (Å$^2$) for Non-Hydrogen Atoms of the $Fe(btz)_2(NCS)_2$ Complex

| | x/a | y/b | z/c | $U_{eq}$[b] |
|---|---|---|---|---|
| | | $T$ = 293 K | | |
| Fe | 5000 | 933 (2) | 2500 | 451 |
| N(1) | 3534 (4) | 650 (3) | 1971 (3) | 469 |
| N(2) | 5221 (5) | −494 (5) | 1613 (4) | 469 |
| N(20) | 5507 (6) | 2260 (7) | 1721 (4) | 677 |
| C(1) | 3498 (6) | −120 (7) | 1404 (4) | 473 |
| C(2) | 4468 (6) | −699 (6) | 1162 (4) | 442 |
| C(3) | 2635 (6) | 1283 (10) | 2266 (6) | 655 |
| C(4) | 1666 (9) | 908 (17) | 1923 (8) | 1435 |
| C(5) | 1487 (9) | 356 (16) | 1290 (10) | 1347 |
| C(8) | 5672 (8) | −2178 (11) | 228 (6) | 712 |
| C(9) | 6181 (8) | −2238 (9) | 1003 (6) | 633 |
| C(10) | 6214 (7) | −1004 (10) | 1426 (7) | 648 |
| C(21) | 5780 (6) | 3125 (8) | 1406 (5) | 496 |
| S(6) | 2453 (2) | −598 (3) | 867 (2) | 735 |
| S(7) | 4412 (2) | −1546 (2) | 289 (1) | 670 |
| S(22) | 6160 (2) | 4359 (2) | 941 (2) | 792 |
| | | $T$ = 130 K | | |
| Fe | 5000 | 776 (2) | 2500 | 205 |
| N(1) | 3620 (5) | 660 (6) | 2011 (4) | 239 |
| N(2) | 5268 (5) | −479 (6) | 1664 (4) | 208 |
| N(20) | 5389 (6) | 2101 (7) | 1756 (4) | 301 |
| C(1) | 3544 (6) | −76 (7) | 1407 (4) | 187 |
| C(2) | 4517 (7) | −687 (7) | 1180 (5) | 238 |
| C(3) | 2729 (6) | 1382 (8) | 2305 (5) | 302 |
| C(4) | 1733 (9) | 1034 (17) | 1959 (8) | 1161 |
| C(5) | 1575 (9) | 626 (15) | 1219 (10) | 1122 |
| C(8) | 5749 (6) | −2177 (8) | 242 (3) | 300 |
| C(9) | 6249 (7) | −2274 (8) | 1051 (5) | 299 |
| C(10) | 6275 (7) | −1022 (8) | 1479 (5) | 287 |
| C(21) | 5642 (6) | 3009 (8) | 1436 (5) | 233 |
| S(6) | 2481 (2) | −447 (2) | 832 (2) | 514 |
| S(7) | 4476 (2) | −1542 (2) | 288 (1) | 365 |
| S(22) | 6048 (2) | 4278 (2) | 972 (2) | 391 |

[a] Numbers in parentheses are estimated standard deviations in the least significant digit. [b] Values for anisotropically refined atoms are given in the form of the isotropic equivalent thermal parameter $U_{eq} = {}^1/_3(U_{11} + U_{22} + U_{33})$.

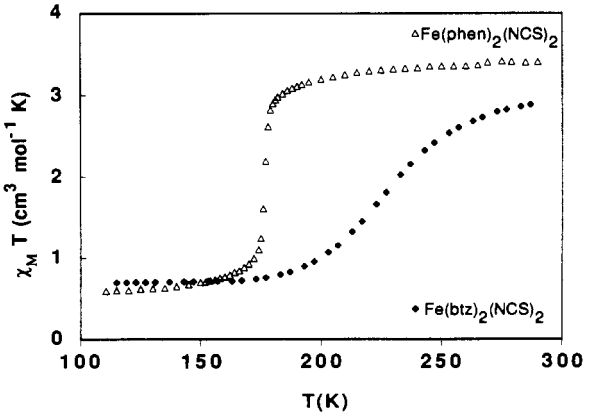


**Figure 1.** Temperature dependence of $\chi_M T$ for a polycrystalline sample of $Fe(btz)_2(NCS)_2$. Data previously reported[4e] for the crystalline form II of $Fe(phen)_2(NCS)_2$ are given for comparison. (For clarity, only the curves obtained at decreasing temperature are drawn.)

curve $\chi_M T$ versus $T$ obtained in the cooling mode is shown in Figure 1, together with one that we recently reported for a crystalline sample of **2**.[4e] Both curves are quite similar to those obtained in the warming mode, and in both cases, the possible hysteresis cannot be wider than 1 K. For **1** the $\chi_M T$ product decreases markedly from 2.90 cm$^3$ mol$^{-1}$ K ($\mu_{eff}$ = 4.81 $\mu_B$) at 295 K and reaches the lower limit of 0.70 cm$^3$ mol$^{-1}$ K ($\mu_{eff}$ = 2.37 $\mu_B$) in the vicinity of 160 K, with about 70% of the spin conversion taking place between 200 and 250 K. These values show that the transition is not complete either at room temperature or at low temperatures. This transition is very similar to that reported by Bradley et al.[6] for a powder sample, but in the latter case it is more complete ($\chi_M T \approx 0.41$ cm$^3$ mol$^{-1}$ K at about 150 K and $\chi_M T \approx 3.06$ cm$^3$ mol$^{-1}$ K at room temperature). The transition of **2** (see Figure 1) is more abrupt than that of **1**. It is centered at 176.5 K. The $\chi_M T$ value is 3.41 cm$^3$ mol$^{-1}$ K ($\mu_{eff}$ = 5.22 $\mu_B$) at 292 K and reaches the lower limit of 0.58 cm$^3$ mol$^{-1}$ K ($\mu_{eff}$ = 2.16 $\mu_B$) in the vicinity of 110 K.

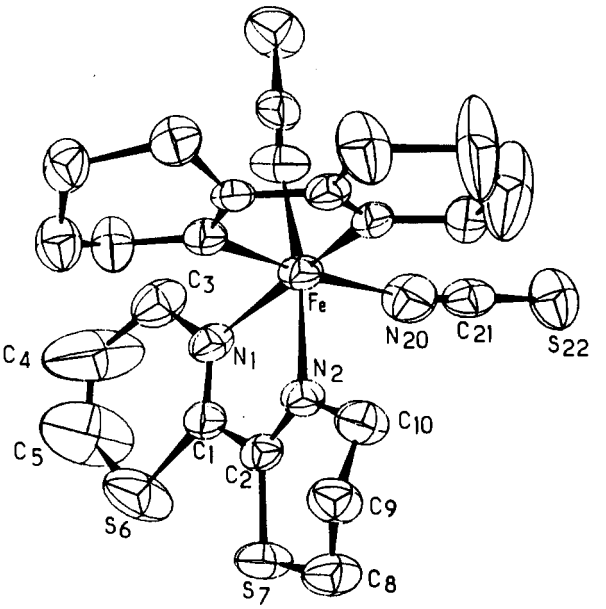


**Figure 2.** Drawing of the $Fe(btz)_2(NCS)_2$ unit, showing the 50% probability ellipsoids at $T \approx 293$ K. Hydrogen atoms have been omitted for clarity.

**Table III.** Bond Lengths (in Å)[a] for **1**

| | $T \sim$ 293 K | $T \sim$ 130 K | | $T \sim$ 293 K | $T \sim$ 130 K |
|---|---|---|---|---|---|
| N(1)–Fe | 2.165 (6) | 1.982 (7) | C(2)–C(1) | 1.491 (10) | 1.477 (11) |
| N(2)–Fe | 2.176 (6) | 1.965 (6) | S(6)–C(1) | 1.740 (7) | 1.733 (8) |
| N(20)–Fe | 2.064 (7) | 1.948 (8) | S(7)–C(2) | 1.742 (7) | 1.746 (9) |
| C(3)–N(1) | 1.466 (9) | 1.479 (11) | C(9)–C(8) | 1.477 (11) | 1.503 (12) |
| C(1)–N(1) | 1.271 (8) | 1.281 (10) | S(7)–C(8) | 1.811 (8) | 1.797 (9) |
| C(2)–N(2) | 1.277 (8) | 1.291 (11) | C(10)–C(9) | 1.518 (11) | 1.515 (11) |
| C(10)–N(2) | 1.466 (10) | 1.469 (11) | S(22)–C(21) | 1.634 (9) | 1.647 (10) |
| C(21)–N(20) | 1.145 (9) | 1.154 (10) | C(4)–C(5) | 1.250 (15) | 1.326 (17) |
| C(4)–C(3) | 1.470 (14) | 1.471 (14) | S(6)–C(5) | 1.798 (11) | 1.767 (12) |

[a] Numbers in parentheses are estimated standard deviations in the least significant digit.

**Description of the $Fe(btz)_2(NCS)_2$ Structures.** As already reported for **2**, no evidence was provided for a change in the *Pbcn* space group over the 293–130 K temperature range. Moreover, the arrangement of units in **1** is quite the same in the low- and high-spin isomers, the most remarkable differences being observed in the intramolecular geometry of the complex.

A perspective drawing of the molecule with the numbering of the atoms included in the asymmetric unit is given in Figure 2. The two $NCS^-$ groups occupy a cis position and correspond to each other, like the two btz ligands, by a 2-fold axis passing through the iron(II) atom. This allows one to point out the chiral character of the molecule. Each unit cell contains two right-handed and two left-handed enantiomers ($Z$ = 4). Interatomic distances and bond angles related to the high-spin ($T \approx 293$ K) and low-spin ($T \approx 130$ K) isomers are listed in Tables III and IV.

Before describing the structures of both isomers, we would emphasize the fact that **1** and **2** are isostructural since they crystallize in the same *Pbcn* space group, with close lattice parameters ($a$ = 13.288 (1) Å, $b$ = 10.861 (1) Å, $c$ = 16.920 (2) Å for **1**; $a$ = 13.161 (2) Å, $b$ = 10.633 (1) Å, $c$ = 17.481 (2) Å for **2**). Moreover, the number of molecules per unit cell is the same ($Z$ = 4). Lastly, as the iron atoms are located on the 2-fold

**Table IV.** Bond Angles (in deg)[a] for **1**

| | $T \approx 293$ K | $T \approx 130$ K |
|---|---|---|
| N(2)–Fe–N(1) | 74.7 (2) | 80.0 (3) |
| N(20)–Fe–N(1) | 97.4 (2) | 91.1 (3) |
| N(20)–Fe–N(2) | 90.7 (2) | 89.7 (3) |
| C(3)–N(1)–Fe | 121.6 (5) | 123.1 (5) |
| C(1)–N(1)–Fe | 116.0 (5) | 115.6 (6) |
| C(1)–N(1)–C(3) | 122.3 (7) | 121.3 (7) |
| C(2)–N(2)–Fe | 115.5 (5) | 115.2 (6) |
| C(10)–N(2)–Fe | 122.6 (5) | 125.2 (5) |
| C(10)–N(2)–C(2) | 120.7 (6) | 118.8 (7) |
| C(21)–N(20)–Fe | 167.7 (6) | 168.0 (7) |
| C(4)–C(3)–N(1) | 116.6 (8) | 115.7 (8) |
| S(6)–C(1)–N(1) | 128.3 (6) | 129.6 (6) |
| C(2)–C(1)–N(1) | 116.9 (6) | 113.9 (7) |
| S(6)–C(1)–C(2) | 114.8 (6) | 116.5 (6) |
| C(1)–C(2)–N(2) | 115.9 (6) | 114.7 (8) |
| S(7)–C(2)–N(2) | 129.2 (6) | 130.3 (7) |
| S(7)–C(2)–C(1) | 114.8 (5) | 115.0 (6) |
| S(7)–C(8)–C(9) | 112.9 (7) | 112.9 (6) |
| C(10)–C(9)–C(8) | 113.1 (7) | 111.9 (7) |
| C(9)–C(10)–N(2) | 114.1 (7) | 115.3 (7) |
| S(22)–C(21)–N(20) | 179.1 (8) | 177.7 (8) |
| S(6)–C(5)–C(4) | 118.7 (1) | 116.6 (11) |
| C(5)–C(4)–C(3) | 129.7 (12) | 125.9 (13) |
| C(5)–S(6)–C(1) | 100.9 (6) | 100.8 (5) |
| C(8)–S(7)–C(2) | 102.1 (4) | 101.8 (4) |

[a] Numbers in parentheses are estimated standard deviations in the least significant digit.

axis in both structures, with nearly equivalent positions ($y/b$ = 0.593 and 0.663 for **1** and **2**, respectively), both complexes will present the same structural packing.

**High-Spin Form Structure ($T \approx 293$ K).** The btz ligands are not planar. If the least-squares plane of each ligand is defined by the N(1), N(2), C(1), and C(2) atoms (equation of the plane: $-0.2355X - 0.7573Y + 0.6092Z = 0.4133$), only the C(3) and C(10) atoms are close to this plane, the strongest deviations being observed for the S(6) and S(7) atoms (deviation: 0.2046 and 0.2266 Å, respectively).

The two ligand rings around the C(1)–C(2) central single bond are distorted. Their configuration, according to the sequence of the torsion angles, is of the 1–2 diplanar form. This is particularly true for the ring including the N(2) atom. In the other ring, the C(4) and C(5) atoms are found to be strongly disordered at room temperature, since $U_{eq}$ = 0.1435 and 0.1347 Å$^2$, respectively (Table II gives their mean statistical fractional coordinates). An attempt to assign two different statistical positions to each of these atoms failed to improve the final least-squares refinement.

Whereas the $NCS^-$ groups are quasi-linear (N(20)–C(21)–S(22) = 178.4°), the Fe–N–C(S) linkages are bent (Fe–N(20)–C(21) = 167.7°). These angular values are very close to those obtained in **2**, the observed deviations being less than 1°.

As already mentioned for other $FeL_2(NCS)_2$ compounds (L = bt, phen, bpy (2,2′-bipyridine) and tap (1,4,5,9-tetraazaphenanthrene)),[4d,4e,17,18] the involved Fe–N(CS) distances (Fe–N(20): 2.064 (7) Å) are shorter than those of the Fe–N(btz) bonds (mean value: 2.175 Å) and the N–Fe–N angles strongly differ from each other:

| | |
|---|---|
| N(1)–Fe–N(2) | 74.7 (2)° |
| N(1)–Fe–N(20) | 97.4 (2)° |
| N(2)–Fe–N(20) | 90.7 (2)° |

These data corroborate the strong distortion which characterizes the high-spin $[FeN_6]$ octahedron in this family of compounds.

A projection of the structure along the $a$ axis is shown in Figure 3. Given the fact that **1** and **2** have the same *Pbcn* space group, the molecular packing may be described similarly as sheets of complex molecules parallel to the $a$–$b$ plane, in which adjacent units, located by the position of the iron atom, alternate along the $b$ direction at the coordinates $x = 0$ and $x = 1/2$.

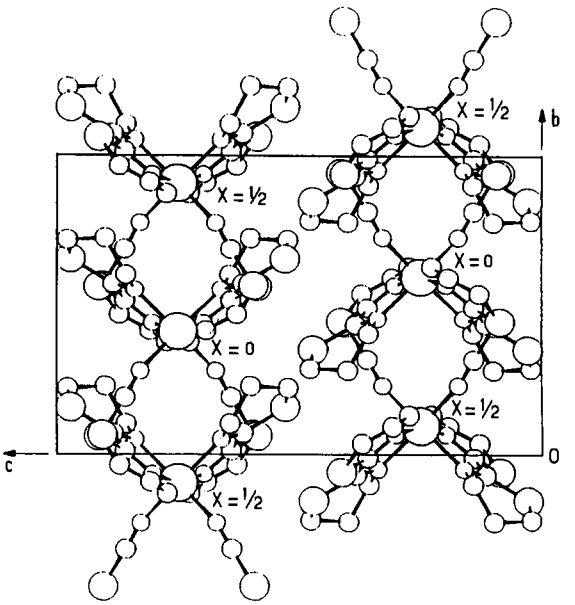


**Figure 3.** Projection of the $Fe(btz)_2(NCS)_2$ crystal structure along the $a$ axis.

**Table V.** Intermolecular Distances (Å) Shorter at $T \approx 130$ K than the van der Waals and Fe···Fe Distance Involved in the Same Interactions[a]

| | $T \approx 293$ K | $T \approx 130$ K |
|---|---|---|
| $C(21)–S(7)_i$ | 3.351 (9) | 3.275 (8) |
| $S(7)–C(21)_i$ | 3.351 (9) | 3.275 (8) |
| $C(8)–C(21)_i$ | 3.523 (12) | 3.451 (10) |
| $C(21)–C(8)_i$ | 3.523 (12) | 3.451 (10) |
| $C(10)–S(22)_{i'}$ | 3.606 (9) | 3.610 (10) |
| $S(22)–C(10)_{i''}$ | 3.606 (9) | 3.610 (10) |
| $S(7)–S(22)_i$ | 3.774 (7) | 3.657 (6) |
| $S(22)–S(7)_i$ | 3.774 (6) | 3.657 (6) |
| $Fe\cdots Fe_i$ | 8.699 (3) | 8.508 (2) |
| $Fe\cdots Fe_{i'}$ | 8.581 (3) | 8.430 (2) |
| $Fe\cdots Fe_{i''}$ | 8.581 (3) | 8.430 (2) |

[a] The first mentioned atom is related to a given central $x$, $y$, $z$ molecule. Small subscript characters give the symmetry operation and the associated translations for the second atom involved in a considered interaction:

| | | |
|---|---|---|
| i | $-x, -y, -z$ | 1,0,0 |
| i′ | $1/2 - x, 1/2 + y, z$ | 1,–1,0 |
| i″ | $1/2 - x, 1/2 + y, z$ | 1,0,0 |

So, intersheet contacts are denoted by i and intrasheet contacts by i′ or i″.

Considering that intermolecular interaction exists if the distance between atoms of adjacent molecules is shorter than the sum of the van der Waals radii, contacts are found (see Table V) between atoms of the btz and $NCS^-$ groups. It should be noticed that interactions between consecutive sheets (e.g. S(7)–C(21) = 3.351 (9) Å, symmetry operation $-X$, $-Y$, $-Z$: 1,0,0) are more pronounced (shorter distances) than the only one observed within a given sheet (C(10)–S(22) = 3.606 (9) Å, symmetry operation $1/2 - X$, $1/2 + Y$, $Z$: 1,–1,0 and 1,0,0).

**Low-Spin Form Structure ($T \approx 130$ K).** The general conformation of the complex is nearly unchanged upon cooling: (i) No significant differences are noted in the intramolecular geometry of the btz ligand. The strongest deviations from the N(1), N(2), C(1), and C(2) least-squares plane (equation of the plane: $-0.2626X - 0.7692Y + 0.5826Z = 0.1873$) still concern the S(6) and S(7) atoms (deviations: 0.1365 and 0.1787 Å, respectively). The configuration of each ring is the same than at room temperature and, at low temperature, the C(4) and C(5) atoms

(17) König, E.; Watson, K. J. *Chem. Phys. Lett.* **1970**, *6*, 457.
(18) Real, J. A.; Muñoz, M. C.; Granier, T.; Gallois, B. Manuscript in preparation.

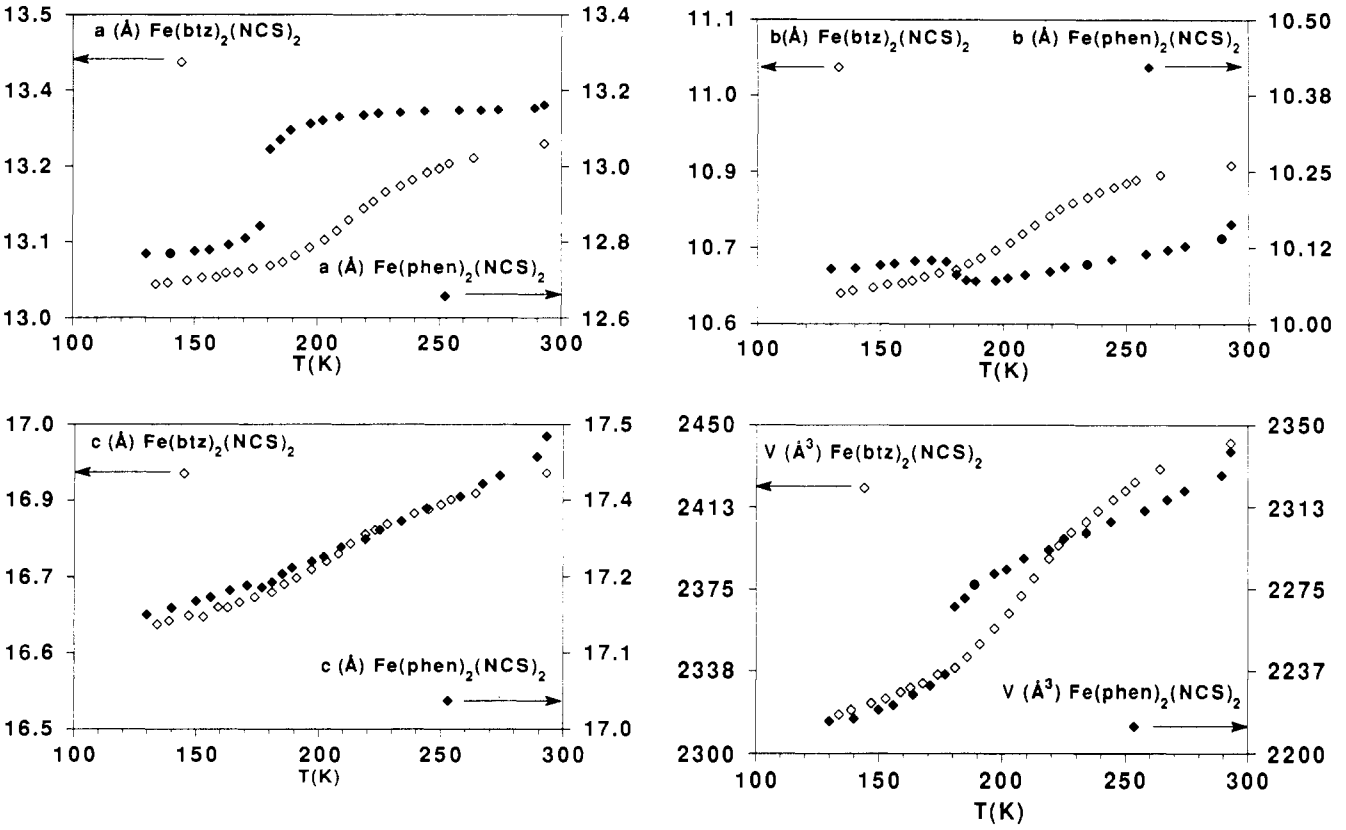


**Figure 4.** Temperature dependence of the lattice parameters of $Fe(btz)_2(NCS)_2$ and $Fe(phen)_2(NCS)_2$.

are still disordered compared with the other C atoms. (ii) The linearity of the $NCS^-$ groups is not affected. These groups are similarly bent with regard to the Fe–N(CS) bonds over the whole temperature range, the small variation of the Fe–N(20)–C(21) angle being insignificant.

As already observed in **2**, the more noticeable intramolecular modifications associated to the spin transition are those which affect the $[FeN_6]$ core geometry. The high-spin → low-spin conversion is characterized by (i) a shortening of the Fe–N distances depending on the nitrogen atom involved in the bonds (the mean Fe–N(btz) bond shortening is reduced by about 0.20 Å, whereas the Fe–N(CS) bond shortening is only about 0.11 Å) and (ii) a variation of the N–Fe–N angles, which are getting closer to 90°:

| | |
|---|---|
| N(1)–Fe–N(2) | 80.0 (3)° |
| N(1)–Fe–N(20) | 96.1 (3)° |
| N(2)–Fe–N(20) | 89.7 (3)° |

The results of these observations is that the $[Fe–N_6]$ core approximates the $O_h$ symmetry much more closely in the low-spin form than in the high-spin form. Moreover, the mean value of the metal–ligand bond length variation, $\Delta R$, is found to be about 0.170 (13) Å, a value which is similar to that (0.164 (6) Å) deduced from the structural description of the high- and low-spin isomers of **2**.

Intermolecular distances shorter than the van der Waals contacts at $T \approx 130$ K, as well as iron–iron distances between the molecules involved in these interactions, are reported in Table V. It is of interest to note that, as at room temperature, the strongest interactions (shortest intermolecular distances) are observed between consecutive sheets in the *c* direction. This observation is reinforced by the fact that a new intersheet contact, involving the S(7) and S(22) atoms, is detected (S(7)···S(22) distance = 3.657 (6) Å). On the contrary, within a sheet, contacts appear to be neither strengthened nor more numerous when passing from 293 to 130 K. Such a behavior differs from that deduced from an analysis of the variations of the intermolecular distances upon cooling in **2**: in that case the most sensitive shortenings affect intermolecular distances within a given sheet.

**Thermal Expansion.** The variation of the lattice parameters *a*, *b*, *c*, and *V* as a function of temperature is shown in Figure 4 for compounds **1** and **2**. The corresponding data are given as supplementary material.

**$Fe(btz)_2(NCS)_2$.** The cell parameters of **1** evolve continuously in the whole temperature range upon cooling. They all show a change of derivative within the 210–215 K region of the spin state conversion. A quantitative analysis of the data leads to relative variations $\Delta a/a$, $\Delta b/b$, and $\Delta c/c$ of 1.9, 1.7, and 1.5%, respectively, between 130 and 293 K. The variation of the unit cell volume is $\Delta V \approx 124$ Å$^3$.

It should be noted that the temperature dependence of each lattice parameter obtained on heating the crystal follows that of the decreasing curve without any noticeable difference, taking into account the accuracy associated to the data.

We have interpolated the experimental data by using suitable polynomials, in order to better follow the effects of temperature variation. The volumic thermal expansion at constant pressure $\alpha = (1/V)(dV/dT)$ is clearly found to increase with temperature up to $T_c = 215 \pm 5$ K, and then to decrease above $T_c$ when temperature tends to the room temperature value. The linear thermal expansions along the cell axes ($\alpha_i = (1/I_i)(dI_i/dT)$) are evaluated (in $K^{-1}$) as follows: $\alpha_a \approx 0.80 \times 10^{-4}$, $\alpha_b \approx 0.74 \times 10^{-4}$, and $\alpha_c \approx 0.72 \times 10^{-4}$ at ≈293 K; $\alpha_a \approx 2.33 \times 10^{-4}$, $\alpha_b \approx 2.42 \times 10^{-4}$, and $\alpha_c \approx 1.40 \times 10^{-4}$ K$^{-1}$ at $\approx T_c$; $\alpha_a \approx 0.47 \times 10^{-4}$, $\alpha_b \approx 0.65 \times 10^{-4}$, and $\alpha_c \approx 0.58 \times 10^{-4}$ at ≈130 K. The relative variations of these parameters lead to the following anisotropy ratios (defined, at a given temperature, from $3\alpha_i/\sum\alpha_i$ values): 1.06:0.98:0.96 at ≈293 K; 1.14:1.18:0.68 at $\approx T_c$; 0.83:1.15:1.03 at ≈130 K. These ratios indicate there is no particular direction along which the structural arrangement is much more affected by temperature effects than in the other directions.

**$Fe(phen)_2(NCS)_2$.** The evolution of the *a* and *b* parameters as a function of temperature strongly differs from the corresponding one observed for **1**. It clearly shows a discontinuity in

the close vicinity of the spin transition. The variations of the two parameters are of different amplitude and of opposite direction.

The *a* parameter decreases slowly when temperature is lowered from 293 K to about 200 K, more and more rapidly between ≈200 and ≈180 K, abruptly from ≈180 to ≈177 K, and then evolves with smaller relative variations as the crystal is cooled down to 130 K. About 58% ($\Delta a \approx 0.21$ Å) of the total variation ($\Delta a \approx 0.39$ Å) occurs in a 4 K range centered on the spin transition temperature and only 20% on the outside of a 30 K range around the same temperature. Such an evolution clearly indicates an abrupt contraction of the unit cell in the *a* direction at $T = 178.5 \pm 1.5$ K.

The amplitude of the overall *b* variation is found to be more limited. The temperature dependence of *b* is smooth and quasi-linear down to about 185 K and below 170 K. However, at the vicinity of the spin transition temperature, it provides evidence for a lattice dilatation ($\Delta b \approx 0.03$ Å) in this direction, which contrasts with the previous *a* contraction.

On the other hand, the evolution of the *c* unit cell parameter reflects the corresponding one in **1**. In this direction, the temperature dependence is continuous over the range 130–293 K, with a change in the derivative sign at the temperature of the spin transition. The overall relative variation $\Delta c/c$ is found to be the same as for **1**, viz. 1.5%.

The variation of the unit cell volume as a function of temperature is correlated with the variation of *a*, *b*, and *c* unit cell parameters. The volume decreases significantly from 293 K to a temperature slightly higher than the transition temperature and then presents a discontinuity when the transition occurs. It is clear that this discontinuity mainly arises from the abrupt contraction of the *a* parameter, limited by the dilatation occurring in the *b* direction. The corresponding drop $\Delta V \approx 31$ Å$^3$ in the 4 K range surrounding the transition temperature is about 26% of the total variation, $\Delta V \approx 119$ Å$^3$.

According to the discontinuities observed for the *a* and *b* unit cell parameters and the unit cell volume, polynomial functions are not appropriate for good reproduction of the experimental data. A good agreement between these data and the calculated values is obtained using a function written in the form $y = a_1 T + a_2 + a_3 \arctan (T - a_4)$, where *y* is the unit cell parameter and $a_i$ ($i = 1$–4) are refinable parameters optimizing the quality of the fit. It should be noted that in such an expression $a_1$, $a_2$, and $a_3$ are dimensionless coefficients whereas $a_4$ expresses the discontinuity temperature. From 293 to 220 K, the contraction amplitude in the *c* direction is more pronounced than in the *a* and *b* directions. Nevertheless, the $\alpha_i$ values being quasi-constant ($\alpha_a \approx 0.22 \times 10^{-4}$, $\alpha_b \approx 0.83 \times 10^{-4}$, and $\alpha_c \approx 1.15 \times 10^{-4}$ K$^{-1}$), the anisotropy ratio (0.30:1.14:1.57 at $T \approx 293$ K) remains nearly unchanged. In the range ≈220–170 K where the spin change occurs, $\alpha_a$ and $\alpha_c$ first increase and then decrease on cooling, whereas $\alpha_b$ shows a reverse evolution. In the close vicinity of the transition, $\alpha_a$ is found to be much larger than $\alpha_c$ and $\alpha_b$ is strongly negative. This reflects the fact that, upon the spin conversion, the lattice contracts predominantly along *a* and expands along *b*. Below $T \approx 170$ K, all the $\alpha_i$ coefficients have positive values, nearly independent of temperature down to 130 K ($\alpha_a \approx 0.72 \times 10^{-4}$, $\alpha_b \approx 0.45 \times 10^{-4}$, and $\alpha_c \approx 0.70 \times 10^{-4}$ K$^{-1}$). The relevant anisotropy ratio is 1.16:0.72:1.12.

## Discussion

**Correlations between Magnetic and Structural Properties.** From magnetic data, both **1** and **2**[4e] compounds are found to present a $^5T \leftrightarrow {}^1A$ spin crossover, with very similar residual fractions $x_{HS}$ of molecules in the high-spin state at low temperature (at $T \approx 130$ K, $x_{HS} \approx 0.20$ in **1** and ≈ 0.17 in **2**) and no noticeable hysteresis effect. The main difference between the magnetic behavior of the two compounds is the sharpness of the transition, gradual for **1** and abrupt for **2**.

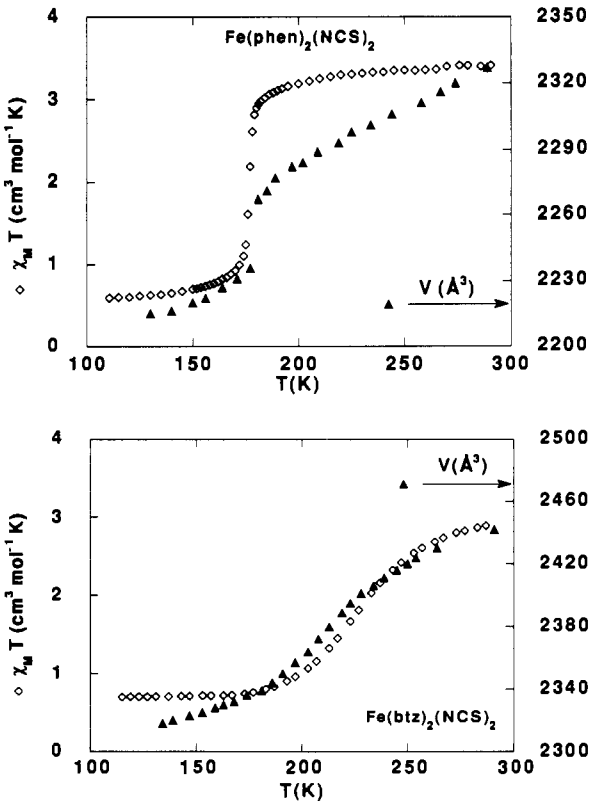


**Figure 5.** Comparison of $\chi_M T$ and *V* variations as a function of temperature for $Fe(btz)_2(NCS)_2$ and $Fe(phen)_2(NCS)_2$.

Owing to the fact that both compounds are isostructural, it is clear that several analogies can be put forward by comparing (see Figure 5) the temperature dependence of the unit cell volume and the $\chi_M T$ versus *T* curve: (i) to the discontinuous spin transition of **2** is associated an abrupt change of the unit cell volume *V*, whereas a continuous evolution of *V* is observed for **1** which exhibits a more gradual spin conversion; (ii) the temperature at which the anomaly (discontinuity, or change of the derivative sign) occurs in the temperature dependence of the lattice volume is in complete agreement with the spin-transition temperature.

These correlations between magnetic properties and thermal dilatation data are reinforced by the fact that the temperature dependence of $\chi_M T$ and of the unit cell parameters obtained upon heating the crystal follows that of the decreasing curve without marked differences.

Nevertheless, from Figure 5, these analogies between $\chi_M T$ and *V* versus *T* variations seem to be no longer valid as far as the $\chi_M T$ value remains constant (temperature range where there is no spin conversion). In fact, in such cases, the evolution of the unit cell volume is only due to the thermal dilatation (contraction) of the lattice, without any contribution resulting from the variation $\Delta R$ of the metal–ligand distances and therefore from the modification of the [Fe–$N_6$] core. This latter point is clearly established, taking into account the structural determination of **2** at $T \approx 193$ K.[19] A close examination of the data, compared to those obtained for the high-spin ($T \approx 293$ K) and low-spin ($T \approx 130$ K) isomers, shows that the [Fe–$N_6$] geometry is the same as the one at room temperature, which is consistent with the magnetic susceptibility measurements indicating no noticeable spin conversion between 293 and 193 K.

In the structural investigation of two analogous iron(II) spin-crossover complexes, Wiehl et al.[20] have successfully expressed the dependence of the lattice dimensions on temperature in terms of the thermal expansion and the deformation tensors associated

(19) Suez-Panamá, F. Ph.D. Thesis, University of Bordeaux I, France, 1991.
(20) Wiehl, L.; Kiel, G.; Köhler, C. P.; Spiering, H.; Gütlich, P. *Inorg. Chem.* **1986**, *25*, 1565.

**Table VI.** Angular Orientations of the Fe–N Bond Directions with Regard to the Principal Axes of the Lattice

| | $Fe(phen)_2(NCS)_2$ | | $Fe(btz)_2(NCS)_2$ | |
|---|---|---|---|---|
| angle, deg | $T \approx 130$ K | $T \approx 293$ K | $T \approx 130$ K | $T \approx 293$ K |
| N(2)–Fe–Ox | 166.1 | 164.3 | 155.4 | 154.1 |
| N(2)–Fe–Oy | 94.6 | 99.9 | 93.5 | 98.2 |
| N(2)–Fe–Oz | 76.9 | 78.0 | 65.7 | 65.6 |
| N(3)–Fe–Ox | 85.7 | 88.3 | 79.7 | 82.2 |
| N(3)–Fe–Oy | 134.0 | 135.5 | 132.9 | 135.4 |
| N(3)–Fe–Oz | 44.3 | 46.6 | 44.8 | 46.4 |
| N(20)–Fe–Ox | 78.6 | 74.7 | 74.8 | 71.0 |
| N(20)–Fe–Oy | 45.3 | 47.4 | 43.5 | 45.8 |
| N(20)–Fe–Oz | 46.9 | 46.6 | 50.4 | 50.4 |

[a] The origin is considered to be on the iron(II) atom.

to the low-spin to high-spin conversion. This development assumes the thermal expansion is the same in both high- and low-spin phases, and was applied in the case of two complexes which exhibit no noticeable residual high-spin fractions at low temperature and similar lattice parameter evolutions in the spin conversion region. An attempt to use a similar description for our compounds failed to reproduce the experimental results. In this case, differences in the thermal expansion coefficients of the two phases imply a more complex expression which includes two different thermal expansion tensors; moreover, one has to introduce corrections which take into account the high-spin residual fraction at low temperature. This new description leads to an increase in the number of parameters to refine in a confident way. In addition, it can be noticed that the *a*, *b*, and *V* parameters of **1** and **2** are far from following the same temperature dependence in the spin-crossover region.

**Structural Changes upon the Spin Transition.** **1** and **2** present very similar structural features in both their high- and low-spin states (same space group and close values of lattice parameters); moreover, the transition is neither associated with a crystallographic phase change nor triggered by a structural order–disorder transition implying for instance the $NCS^-$ groups. Evidence is only provided for a large rearrangement of the iron atom environment without any reorientation of the $[Fe–N_6]$ core which might have explained, at least for **2**, the abrupt variations of the *a* and *b* parameters (the Fe–N bond directions with regard to the unit cell axes are nearly the same for both spin form of **1** and **2** (see Table VI)). In the temperature range of the spin change, the evolution of the unit cell parameters *a*, *b*, and *c* of **1** and *a* and *b* of **2** closely follows the respective $\chi_M T$ vs *T* curves. The continuous variation of *c* observed for **2** in spite of the discontinuous character of the transition may be accounted for by the fact that, in this compound, the spin conversion is expected to mainly propagate perpendicularly to the *c* direction (since most of the intermolecular interactions are observed within sheets parallel to the (110) plane.[4c]

Let us now consider the intramolecular changes associated with the spin transition. As neither the intramolecular geometry of the btz and phen ligands nor the linearity of the $NCS^-$ groups is noticeably affected, the most significant variations observed for both compounds concern the geometry of the $[Fe–N_6]$ octahedron. Below the spin transition temperature, not only are the N–Fe–N angles closer to 90° but the differences noted in the Fe–N bond lengths of the high-spin isomer significantly decrease. Largely distorted in the high-spin state, the $[Fe–N_6]$ coordination core is thus more regular in the low-spin state.

More precisely, a strong similarity is observed between **1** and **2** concerning the reduction of the metal–ligand bond lengths in the 293–130 K range. The shortening of the Fe–N(CS) distances (0.11 and 0.10 Å, respectively) and that of the mean Fe–N(btz, phen) distances (0.20 Å) are comparable, which results in close values for the average variations ($\Delta R$) of these distances (about 0.170 and 0.164 Å, respectively). However, as seen above, both spin crossovers are incomplete at low temperature. Moreover, at room temperature, **1** contains ≈15% of the low-spin form. It follows that the change in $\Delta R$ associated with a complete spin conversion can be estimated at ≈0.26 Å for **1** and 0.20 Å for **2**. This shows that, in the present case, the difference in sharpness of the transitions does not depend on $\Delta R$.

Although these latter values are in fair agreement with those reported (0.19 ± 0.05 Å) for $S = 0 \leftrightarrow S = 2$ conversions in the iron(II) spin-crossover complexes with a $[Fe–N_6]$ coordination core,[4c] their relative magnitude sets the problem of their direct influence on the spin-transition characteristics. In a previous description of the structural changes associated with the spin transition in **2**,[4c] we underlined the fact that the $\Delta R$ value obtained for this crystalline form of $Fe(phen)_2(NCS)_2$ (form II) was lower than that reported for the crystalline form I ("extracted sample"), the transition of which is more abrupt than that of the form II. If $\Delta R$ were the main parameter governing the spin-crossover cooperativity, the transition sharpness should be rather similar for **1** and **2**. Magnetic measurements indicate that this is not the case. So, if $\Delta R$ is certainly a relevant parameter to account for the more or less gradual character of spin transitions, it clearly appears that it is not the only one. It is well-known that cooperative effects involve a distortion at one site, which may be imparted to the neighboring sites via intermolecular coupling. It follows that factors such as intermolecular contacts, as well as the anisotropy or the rigidity of the systems, are expected to play a role.

**Volume Changes as a Function of Temperature.** Despite the difference in cooperativity of the spin-crossovers of **1** and **2**, the variation $\Delta V$ of the unit-cell volume between 293 and 130 K is found to be similar for both compounds ($\Delta V \approx 124$ Å$^3$ for **1** and 119 Å$^3$ for **2**), which corresponds to $\Delta V/V \approx 5.1\%$ in each case. Nevertheless, this observation cannot be directly taken into account since $\Delta V$ is the sum of two contributions: the volume change $\Delta V_{SC}$ resulting from the spin crossover and the lattice thermal expansion $\Delta V_T$. From Figure 4 it is easy to estimate $\Delta V_{SC}$ and $\Delta V_T$: $\Delta V_{SC} \approx 58$ Å$^3$ and $\Delta V_T \approx 66$ Å$^3$ for **1**; $\Delta V_{SC} \approx 60$ Å$^3$ and $\Delta V_T \approx 59$ Å$^3$ for **2**. So the $\Delta V$, $\Delta V_{SC}$, and $\Delta V_T$ values obtained for the two species are very close to each other.

Concerning $\Delta V_{SC}$, the values associated with a complete spin conversion can be estimated at ≈89 Å$^3$ for **1** and ≈72 Å$^3$ for **2**, i.e. ≈22 and ≈18 Å$^3$ per formula unit, respectively. Taking into consideration the uncertainties on these data, it clearly appears that $\Delta V_{SC}$ is not a relevant parameter to account for the more or less cooperative character of the spin crossover of the two iron(II) complexes. This statement seems all the more legitimate as the values obtained for **1**, which presents the most gradual spin change, are higher than those obtained for **2**.

The same conclusion holds for the parameter $\Delta V_T$. The similarity of the $\Delta V_T$ values relative to **1** and **2** is reflected by the fact that, in the temperature ranges where no noticeable spin change occurs, the volumic $\alpha$ coefficients are found to be close for the two compounds (at ≈293 K, $\alpha = 2.26 \times 10^{-4}$ K$^{-1}$ for **1** and $2.20 \times 10^{-4}$ K$^{-1}$ for **2**; at ≈130 K, $\alpha = 1.70 \times 10^{-4}$ K$^{-1}$ for **1** and $1.87 \times 10^{-4}$ K$^{-1}$ for **2**.

**Intermolecular Contacts and Anisotropy.** In both complexes, the molecular packing can be similarly described as sheets of molecules parallel to the *a*–*b* plane. However, the intermolecular interactions and their modification upon the spin change are found to widely differ.

In **1**, the intrasheet contacts only involve the C(10) and S(22) atoms of neighboring molecules. They are very weak and do not noticeably vary with temperature. The intersheet contacts mainly form between C(21) and S(7) or C(8) atoms. They are strong and are reinforced upon the high-spin to low-spin conversion.

In **2**, two types of intrasheet interactions exist at room temperature. They are of the type C(4)···C(9) and C(3)···C(7).

At about 130 K, four other types of contacts appear between the carbon atoms of two neighboring molecules. On the other hand, only one intersheet contact is observed. It forms between C(7) and S(22) atoms and is nearly as strong at 130 K as at 293 K.

These data lead to the following comments: (i) the intersheet interactions are stronger than the intrasheet ones; (ii) the intermolecular contacts at room temperature and their reinforcement at low temperature are essentially intersheet for **1** and intrasheet for **2**; (iii) the increase in the number of contacts when passing from the high-spin to the low-spin form is much more pronounced for **2** than for **1**.

It is worth underlining that the bidimensional character and, consequently, the anisotropy of the structure are more marked in **2** than in **1**. This is illustrated by the relative values of the linear thermal expansion coefficients $\alpha_a$, $\alpha_b$, and $\alpha_c$, in the temperature ranges where no noticeable spin conversion occurs. Actually, the corresponding anisotropy ratios are found to be 0.30:1.14:1.57 at ≈293 K and 1.16:0.72:1.12 at ≈ 130 K for **2**, which is indicative of a large expansion anisotropy, principally at room temperature, while they are close to each oter at a given temperature for **1** (e.g. 1.06:0.98:0.96 at ≈293 K and 0.83:1.15:1.03 at ≈ 130 K), which characterizes a significant tridimensional character.

## Conclusion

The above discussion, concerning the comparison between the volumic and structural changes thermally induced in compounds **1** and **2**, which exhibit gradual and discontinuous spin crossovers, respectively, can be summarized as follows. For both complexes, the space group is the same and is not modified upon the spin crossover. The molecular packing is similar. The variations of the mean metal–ligand bond length as well as those of the unit cell volumes associated with the high-spin ↔ low-spin full conversion are close. The volume changes only resulting from the lattice thermal expansion are also found to be comparable. So, it seems that $\Delta R$, $\Delta V_{SC}$, $\Delta V_T$ are not relevant parameters to account for the difference in sharpness of the spin crossovers of **1** and **2**.

From the above results, it follows that the key factors governing the cooperativity of the process might be, in the present cases, (i) the number and the strength of the intermolecular interactions[4d] and/or (ii) the anisotropy of the lattice expansion.[21]

**Acknowledgment.** This work was partially supported by the Comision Interministerial de Ciencia y Tecnología (Project PB88-0490) and the Acciones Concertadas de Investigación Universitaria (Universitat de València). We thank A. Filhol (Institut Laue Langevin, Grenoble, France) for friendly and fruitful discussions as well as for providing an unpublished software thermal expansion analysis.

**Supplementary Material Available:** Table SII, thermal variation of the lattice parameters, measured on cooling and warming modes, in the 130–293 K temperature range for compounds **1** (a) and **2** (b), respectively (4 pages). Ordering information is given on any current masthead page.

(21) Adler, P.; Wiehl, L.; Meissner, E.; Köhler, C. P.; Spiering, H.; Gütlich, P. J. *Phys. Chem. Solids* **1987**, *48*, 517.